BLENDS OF POLY(VINYL PYRIDINE)S AND DIHYDRIC PHENOLS: THERMAL AND INFRARED SPECTROSCOPIC STUDIES. PART V

NICOLÁS GATICA[*], *FRANCISCO MEDINA, CONSTANZA MORAGA AND LORETO VERGARA*

Department of Polymers, Faculty of Chemical Sciences, University of Concepción, P.O. Box 160-C, Concepción, Chile.

ABSTRACT

Binary blends with poly(4-vinyl pyridine) (P4VPy) 160,000 g/mol and poly(2-vinyl pyridine) (P2VPy) 159,000 g/mol as polymer components and 4,4´-thiodiphenol (TDP), 4,4´-methylendiphenol (MDP), 2,2´-biphenol (22BP) and 4,4´-biphenol (44BP) as low molecular weight compounds (LMWCs), were prepared. Miscibility between the components was analyzed by Fourier Transform Infrared Spectroscopy (FTIR) and Differential Scanning Calorimetry (DSC). Thermogravimetric Analysis (TGA) and Scanning Electron Microscopy (SEM) were also used as complementary techniques. Hydrogen bonding formation was detected by FTIR due to the increasing of the wave number corresponding to the deformation absorption of pyridine groups in P4VPy and P2VPy. A decreasing of melting points and fusion heats of the LMWCs is observed by DSC, which shows a lower crystallinity level as the blends are richer in the polymer component as a consequence of the intermolecular interaction. A plasticizing effect is also observed by DSC when P4VPy is blended with TDP and MDP; the higher steric hindrance prevents this effect when P2VPy is blended with 22BP and 44BP. Miscible blends were obtained with a moderate trend to a higher interaction degree in blends containing P4VPy. This report is the fifth part of a series of works including polymer-LMWC blends. Variables such as molecular weight increase in P4VPy and steric hindrance in P2VPy have been comparatively analyzed with blends previously reported.

Keywords: Polymer blends, poly(vinylpyridine)s, low molecular weight compounds, hydrogen bond, miscibility.

INTRODUCTION

In the last decades, a significant development of different kinds of polymeric materials has been reported: homo- and co-polymers, miscible and immiscible polymer blends, polymer emulsions and suspensions, and blends formed by a polymer and a low molecular weight compound (LMWC) [1-11]. A cross-cutting goal in these works is to improve the properties of the obtained products. In the case of polymer-polymer blends, the obtaining of materials with enhanced properties is supported by the fundamental characterization of the intermolecular interactions involving a series of different functional groups, namely: methacrylic acid and ether groups [12], 4-vinylphenol and 2-ethoxyethyl methacrylate [13], itaconamic acids and 2-vinylpyridine [14], aryl esters [15], lactam group [16], lactide and styrene [17], vinyl methyl ether and methyl methacrylate [18], ethylene oxide and vinyl alcohol [19], aniline and amide groups [20] and alkylstyrenes and isoprene [21], among others. In this way it has been possible to find many applications involving polymer-polymer blends [22-25] and re-using preexisting polymeric materials [6,25,26-28]. Biodegradable polymer blends have also attracted increasing attention in recent years [24,29]. In the field of the polymer-LMWC blends, many works are focused on possible applications and not so much on the molecular characterization of interactions. LMWCs are added as additives to improve the properties of the polymeric component [6,30-37]. Consequently, polymer- LMWC blends with different practical applications have been reported: controlled drug devices [38-42], regenerative medicine [43], electronic devices [44], hemodialysis applications [45], etc. In addition, LMWCs have been used not only as blend components but also as blend compatibilizers [46-49].

The corresponding author and co-workers have reported a series of works dealing with functional vinyl polymers [50-53] such as poly(4-vinyl pyridine) (P4VPy) and poly(2-vinyl pyridine) (P2VPy) as polymer components and dihydric phenols as low molecular weight components. The monomer units 4-vinyl pyridine and 2-vinyl pyridine are proton acceptor groups that can interact with proton donor groups such as phenolic units. P4VPy and P2VPy with lower molecular weights have been previously studied in our laboratory as polymer components of blends.

This work is aimed to present the blending behavior of binary systems formed by P4VPy 160,000 g/mol and P2VPy 159,000 g/mol as polymer components and 4,4´-thiodiphenol (TDP), 4,4´-methylendiphenol (MDP), 4,4´-biphenol (44BP) and 2,2´-biphenol (22BP) as LMWCs. The structural formulas of P4VPy, P2VPy, TDP, MDP, 44BP and 22BP are shown in Figure 1. The blends P4VPy/TDP, P4VPy/MDP, P2VPy/22BP and P2VPy/44BP were studied by Fourier Transform Infrared Spectroscopy (FTIR), Differential Scanning Calorimetry (DSC), Thermogravimetric Analysis (TGA) and Scanning Electron Microscopy (SEM).

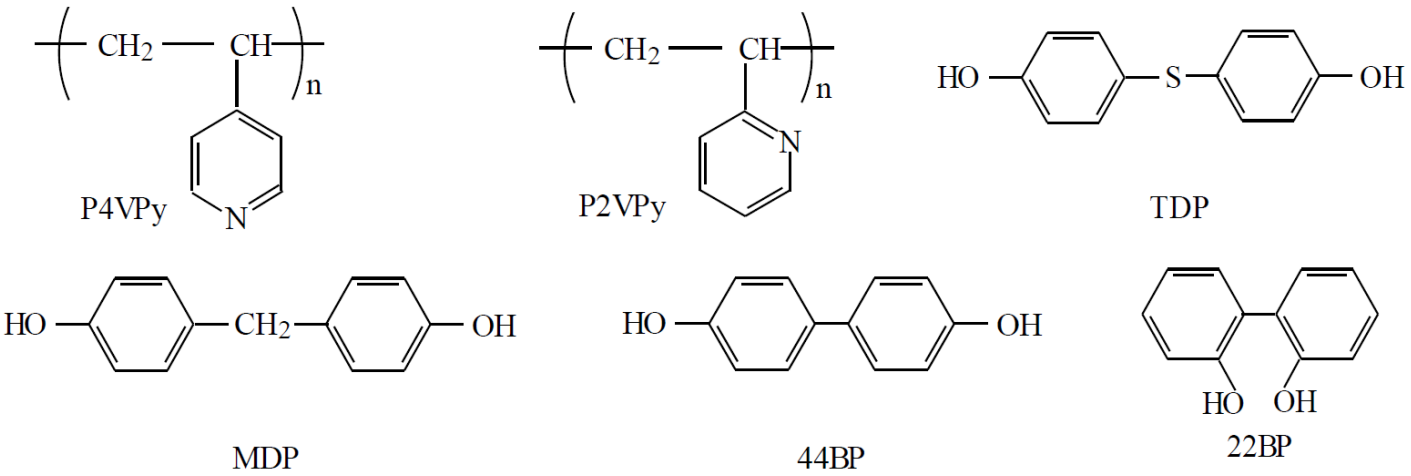

Figure 1. Structural formulas of poly(4-vinyl pyridine) (P4VPy), poly(2-vinyl pyridine) (P2VPy), 4,4´-thiodiphenol (TDP), 4,4´-methylendiphenol (MDP), 4,4´-biphenol (44BP) and 2,2´-biphenol (22BP).

email: nicolasgatica@udec.cl

EXPERIMENTAL

Blend components

Aldrich's P4VPy, P2VPy, TDP, MDP, 44BP and 22BP were used. The weight-average molecular weights (Mw) of P4VPy and P2VPy are 160,000 and 159,000 g/mol respectively. Melting points (Tm) of TDP, MDP, 44BP and 22BP are 151.6, 160.7, 281.5 and 109.9 ºC respectively.

Preparation of blends

Blends of different compositions were obtained by solution casting using methanol as solvent. From mother solutions of the pure components, blends were prepared in Petri dishes with stirring of about 12 h. After that, the solvent was evaporated at room temperature. Finally, samples were vacuum dried at room temperature for about two weeks until constant weight. The blend concentration was about 2 weight %.

Table 1 shows the compositions and denomination of the blends included in this work.

Table 1. Composition and denomination of the studied blends.

Blend	Composition (weight % in LMWC)	Correlative denomination
P4VPy + TDP (A)	0, 10, 20, 30, 40, 50, 60, 70, 80, 90, 100	1A, 2A, 3A, 4A, 5A, 6A, 7A, 8A, 9A, 10A, 11A
P4VPy + MDP (B)	0, 10, 20, 30, 40, 50, 60, 70, 80, 90, 100	1B, 2B, 3B, 4B, 5B, 6B, 7B, 8B, 9B, 10B, 11B
P2VPy + 22BP (C)	0, 10, 20, 30, 40, 50, 60, 70, 80, 90, 100	1C, 2C, 3C, 4C, 5C, 6C, 7C, 8C, 9C, 10C, 11C
P2VPy + 44BP (D)	0, 10, 20, 30, 40, 50, 60, 70, 80, 90, 100	1D, 2D, 3D, 4D, 5D, 6D, 7D, 8D, 9D, 10D, 11D

FTIR spectra

Infrared spectra of P4VPy, P2VPy, TDP, MDP, 22BP, 44BP and their blends were recorded on a Nicolet Magna IR 550 Fourier transform infrared spectrophotometer. Spectra were recorded with a resolution of 1 cm^{-1}. Samples were prepared directly in KBr pellets.

DSC measurements

The glass transition temperature (Tg) of P4VPy, P2VPy and blends and the melting temperatures (Tm) of TDP, MDP, 22BP, 44BP and blends were obtained by Differential Scanning Calorimetry (DSC) from the thermograms registered with a differential scanning calorimeter Netzsch DSC 201 F1 Phoenix. Samples (3-5 mg) were placed inside aluminum pans and heated under flowing nitrogen (80 mL/min), ranging from 20 to 200 ºC for blends A, B and C and from 20 to 320 ºC for blend D, at 10 (ºC/min).

In order to minimize differences in the thermal history of the samples, the corresponding thermograms were obtained according to the following temperature program: heating up to T_1 temperature (dynamic stage), isothermal stage at T_1 (static), cooling until the initial temperature (dynamic, quenching step), isothermal step at the initial temperature (static) and heating until the final temperature (dynamic) [T_1 = 200 ºC for blends A and B and T_1 = 80 ºC and 180 ºC for blends C and D respectively; final temperature = 200 ºC for blends A and B, and final temperature = 200 ºC and 300 ºC for blends C and D respectively]. In all cases, Tg, Tm and the heat of fusion (ΔH_{fus}) were evaluated from the last stage.

Samples were dried under reduced pressure in a vacuum oven prior to measurements.

TGA measurements

Thermogravimetric measurements were performed using a Netzsch TG 209 F1 Iris thermo micro balance. Samples (3-5 mg) were placed inside aluminum pans and heated under flowing nitrogen (20 mL/min) ranging from 25 to 550 ºC at 10 ºC/min, obtaining the corresponding thermal decomposition profiles. Samples were dried under reduced pressure in a vacuum oven prior to measurements.

SEM micrographs

Samples were prepared according to the procedure described in the Preparation of blends section. Furthermore, a glass slide was deposited in the Petri dish, which was removed and kept at room temperature to allow the total solvent evaporation and the formation of an appropriate film for this technique. Samples were metalized by deposition of gold ions to allow the samples were conductive. Required magnifications were programmed by means of the microscope software and the images were obtained by means of a scanning electron microscope JEOL JSM 6380 LV.

RESULTS AND DISCUSSION

Historically, several procedures have been used for characterizing blends containing polymers. One of the analytical techniques most required for these purposes is the infrared spectroscopy [2,3,12-19,44,50-53], which is particularly useful to identify the kind of intermolecular interactions responsible for the miscibility between the components. A shifting in the wave number of the characteristic IR absorption bands associated to determined functional groups, can be attributed to intermolecular association [3,14-17,50-53].

Figure 2 shows the FTIR spectra for the compositions 1, 3, 5, 7, 9 and 11 of blends A and B, as representative examples. Characteristic bands corresponding to the blend components are observed such as the stretching vibrations of: O-H phenol (around 3300 cm^{-1}), C=C arene (around 1600 cm^{-1}) and C-O phenol (around 1250 cm^{-1}).

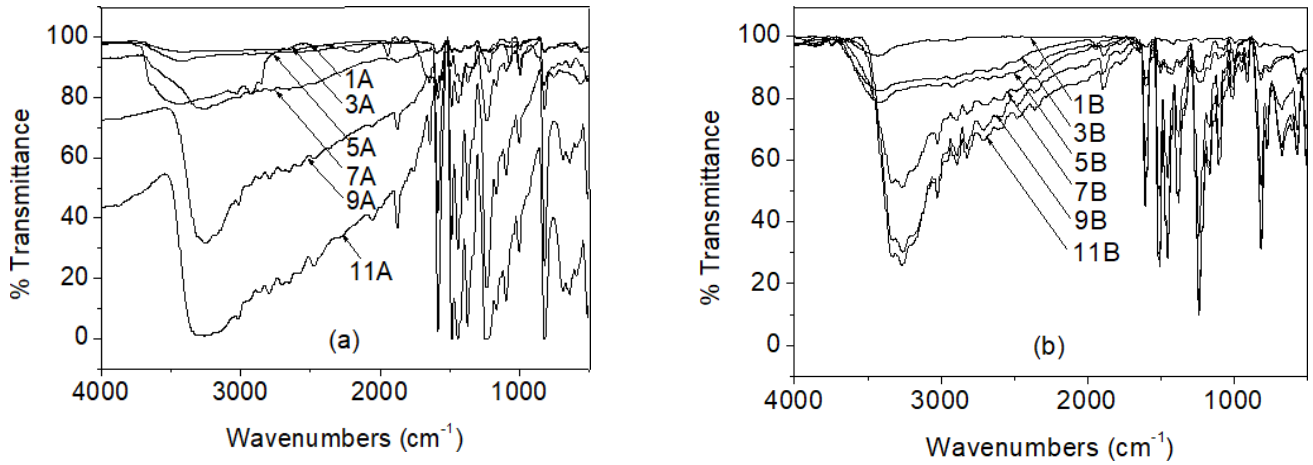

Figure 2. FTIR spectra for blends a) A and b) B (compositions 1, 3, 5, 7, 9 and 11).

A first indication of intermolecular interaction is the position of the O-H stretch band, which can be attributed to associated O-H groups compared to unassociated O-H functions, which appear above 3600 cm^{-1} [54]. However, this band is not sufficiently reliable due to its width and can be also confused with other vibrational modes; in this case, hydrocarbon C-H stretching from P4VPy and P2VPy. For these reasons, another signal was chosen: monomer units of both polymers contain pyridine groups, which show bands corresponding to the ring deformation around 993-994 cm^{-1} and none of the LMWCs has pyridinic rings. This vibrational mode experiences a shifting to higher wave numbers when is forming a hydrogen bonding, which is attributed to a increasing of the associated ring stiffness [50-53,55]. Figure 3 shows the wave number corresponding to the deformation absorption of pyridine groups in P4VPy and P2VPy in relation to the composition for blends A, B, C and D.

In every case, an increasing of the wave number is observed to the extent that the blend is enriched in LMWC. A higher content of TDP, MDP, 22BP and 44BP implies a higher content of hydroxyl groups available for the hydrogen bonding with the polymers. All LMWCs have hydroxyl groups linked to aromatic rings, which have a significant trend to hydrogen bonding formation [50-53,56,57] due to their proton-donor nature. P4VPy and P2VPy, for their part, contribute with pyridinic rings which show a high trend to accept protons [14,51,52,55]. Thus, the intermolecular interaction originates more rigid pyridinic rings and, consequently, a higher energy amount is needed to deform them. This behavior has been reported earlier for other polymer blends containing poly(vinylpyridine)s [51,52,55].

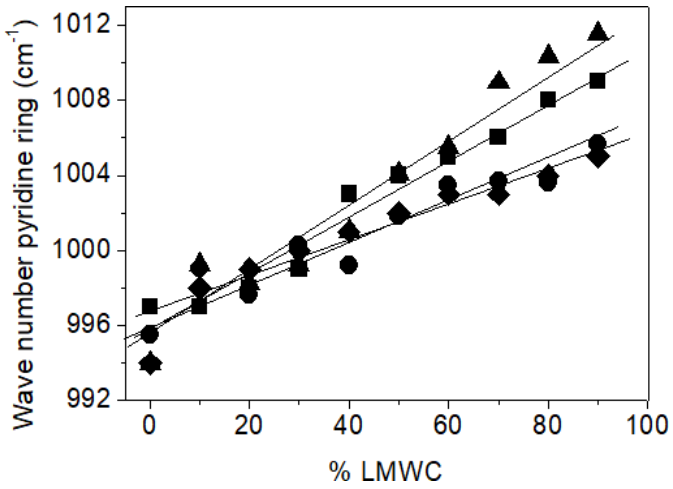

Figure 3. Wave number corresponding to the deformation absorption of the pyridine groups in the blends A (■), B (▲), C (◆) and D (●).

Another interesting result is observed in Figure 3: higher wave number values are obtained for blends A and B in relation to blends C and D as the content of LMWC increases. Functional groups are the same in all cases, i.e. pyridine rings in polymer components and hydroxyl groups linked to aromatic rings in LMWCs and the electronic environment is therefore the same one. The difference observed reflects the spatial distribution of the functional groups involved in the interaction, behavior previously reported for similar systems [51]. In P4VPy (blends A and B) each nitrogen atom is in *para*-position with respect to the main chain of the polymer, that is, a better spatial position for interacting. In P2VPy (blends C and D) each nitrogen atom is in *ortho*-position and, therefore, more sterically hindered.

As a way to corroborate this spectroscopic behavior observed in blends A, B, C and D, the following additional results are presented. These were obtained for blends formed by P4VPy 160,000 g/mol as polymer component and 22BP and 44BP as LMWCs. Figure 4 shows the variation of the pyridine ring wave number with the composition: a displacement of this band towards higher values is also observed as the blend becomes richer in LMWC. In addition, in the case of blend P4VPy/44BP, higher wave number values are obtained as the content of 44BP increases. As discussed, these results demonstrates a higher degree of intermolecular interaction between the components, favored in this case by a better spatial accessibility of the phenolic oxygen in 44BP compared with 22BP.

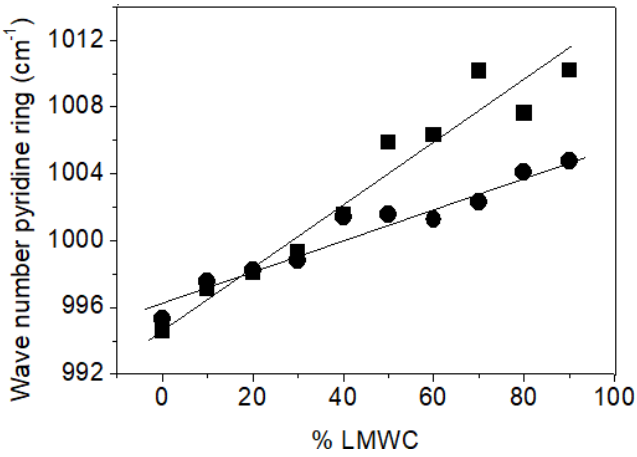

Figure 4. Wave number corresponding to the deformation absorption of pyridine groups in blends of P4VPy with 44BP (■) and with 22BP (●).

Figure 5 shows the thermograms corresponding to the A and B series obtained according to the procedure described in DSC measurements. From these curves, glass transition temperature (Tg), melting temperature (Tm) and heat of fusion (ΔH_{fus}) values were evaluated and collected in Table 2.

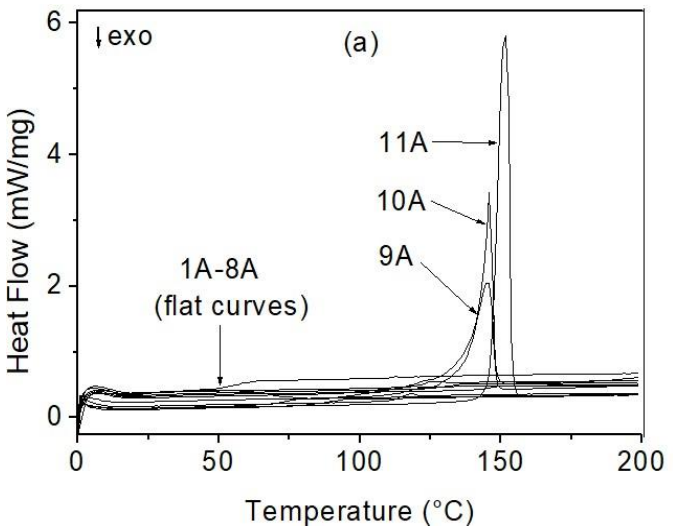

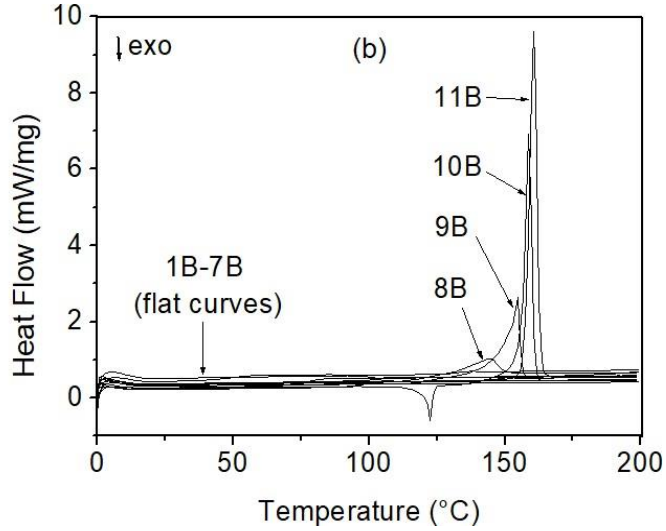

Figure 5. Thermograms of a) A blend and b) B blend.

Table 2. Glass transition temperature (Tg), melting temperature (Tm) and heat of fusion (ΔH_{fus}) for blends A and B.

Sample blend A	Tg (°C)	Tm (°C)	ΔH_{fus} (kJ/mol TDP)	Sample blend B	Tg (°C)	Tm (°C)	ΔH_{fus} (kJ/mol MDP)
1A	142.5	-	-	1B	142.5	-	-
2A	127.5	-	-	2B	128.0	-	-
3A	118.0	-	-	3B	114.5	-	-
4A	108.0	-	-	4B	97.0	-	-
5A	101.0	-	-	5B	88.5	-	-
6A	84.0	-	-	6B	76.0	-	-
7A	69.0	-	-	7B	69.0	-	-
8A	54.5	-	-	8B	-	144.3	11.6
9A	-	145.4	25.6	9B	-	154.8	24.6
10A	-	146.2	26.6	10B	-	158.8	31.0
11A	-	151.6	35.6	11B	-	160.7	37.8

For blends A and B, a shifting of the glass transition temperatures to lower values is registered as the content of TDP or MDP increases. An evident *plasticizing effect*, described in several polymer blends previously studied [32,50-53], is observed, that is, the reduction of the Tg corresponding to the polymer component: the material becomes more flexible, improving the malleability for further use [6]. The LMWC acting as plasticizing increases the *free volume* between the polymer chains and so less energy is required to produce motion on chain segments. Thus, the glass transition temperature decreases.

As shown in Figure 5-a for blend A, melting peaks are obtained only for samples 11A (100% TDP), 10A (10% P4VPy) and 9A (20% P4VPy). No melting signals were registered for the interval 8A (30% P4VPy) - 1A (100% P4VPy), which can be interpreted in terms of the effect of P4VPy over TDP crystallization. From 30% P4VPy, intermolecular interactions produce a disorder material at the molecular level and therefore melting processes of TDP are prevented.

Sample 11A shows Tm = 151.6 °C, which changes to 146.2 °C and 145.4 °C for 10A and 9A respectively. Consequently, heats of fusion (ΔH_{fus}) determined from the corresponding melting peaks, are 35.6, 26.6 and 25.6 (kJ/mol TDP) for 11A, 10A and 9A respectively.

A lower amount of energy must be supplied for melting TDP as the blend is richer in P4VPy. As a result of the intermolecular interactions, crystallinity of TDP decreases with the polymer content until blend exists in amorphous state from composition 8A (30 % P4VPy). A trend to decreasing of Tm and ΔH_{fus} with the increasing of the P4VPy % is also observed for blend B (Table 2). Similar results were previously reported by our laboratory for equivalent systems formed by P4VPy with Mw = 60,000 g/mol, as polymer component [51] under identical experimental conditions. In other words, a high enough level of intermolecular interactions is maintained to generate miscible systems, in spite of the increasing of the molecular weight, in this case from 60,000 to 160,000 g/mol. The strength of the specific interactions such as hydrogen bonding, is capable to counteract the increasing of the molecular weight, an unfavorable factor in any polymeric miscibilization process.

Table 3 collects calorimetric parameters for blends C and D. The same behavior is observed for Tm and ΔH_{fus}: lower values from 11C and 11D until 7C and 5D in so far as the polymer content increases. Cristallinity of 22BP and 44BP diminishes by the intermolecular interactions with P2VPy and so less energy is required to melt the blend.

Table 3. Glass transition temperature (Tg), melting temperature (Tm) and heat of fusion (ΔH_{fus}) for blends C and D.

Sample blend C	Tg (°C)	Tm (°C)	ΔH_{fus} (kJ/mol 22BP)	Sample blend D	Tg (°C)	Tm (°C)	ΔH_{fus} (kJ/mol 44BP)
1C	-	-	-	1D	99.0	-	-
2C	-	-	-	2D	100.0	-	-
3C	-	-	-	3D	102.5	-	-
4C	-	-	-	4D	102.0	-	-
5C	-	-	-	5D	101.0	230.6	4.9
6C	-	-	-	6D	102.5	256.0	16.7
7C	-	95.6	0.2	7D	106.0	270.8	26.5
8C	-	101.3	3.7	8D	100.5	275.5	35.3
9C	-	106.2	10.1	9D	102.0	278.3	37.7
10C	-	106.8	12.9	10D	-	279.6	41.8
11C	-	109.9	21.0	11D	-	281.5	49.6

According to Table 3, two differences can be observed in blends C and D in relation to blends A and B. No Tg signals are obtained for C, which can be a consequence of the Tg value corresponding to P2VPy is close to the Tm value of 22BP, making it difficult to determine. It can be also observed that the Tg for blend D keeps practically constant for different compositions, that is, no plasticizing effect is obtained. This experimental result may reflect a lower level of interaction as a consequence of position of the nitrogen atom in the P2VPy with a higher steric hindrance. Therefore, the results obtained by DSC confirm the behavior observed by FTIR: miscibility between the components in all the systems studied, with a trend to a higher level of intermolecular affinity in blends A and B.

In Figure 6 the thermal decomposition profiles for blends A and B are shown as representative examples. Intermediate decomposition profiles were obtained for the different blend compositions compared to the pure components, which can be considered as an additional base of miscibility, as it has been reported for other polymer blends by the authors [50-53]. The same behavior was registered for blends C and D.

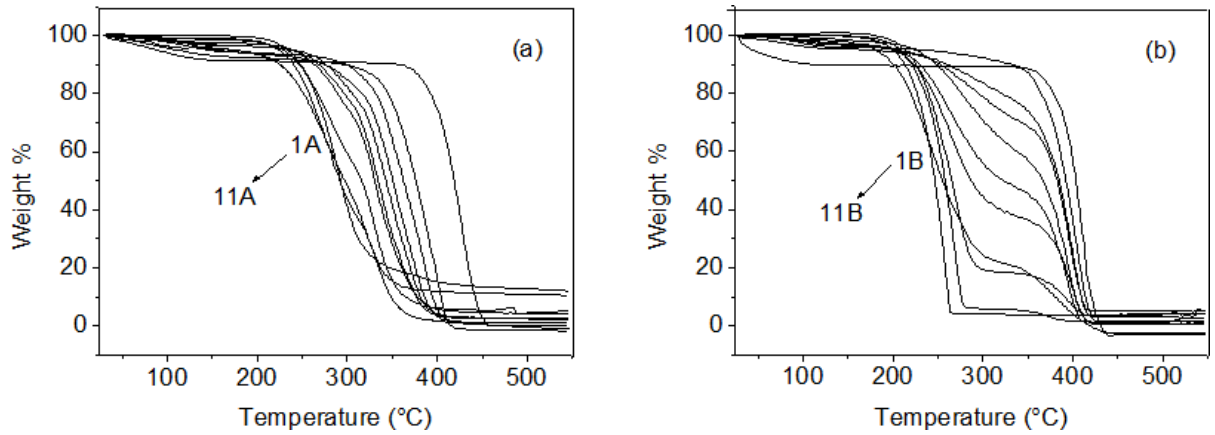

Figure 6. Thermal decomposition profiles of blends a) A and b) B.

From the curves shown in Figure 5, different stability parameters were evaluated: initial decomposition temperature (Ti), temperature at which the weight reduction reaches 50 % (T50) and residual weight % (res %). Ti, T50 and res % values obtained for blends A, B, C and D are collected in Table 4.

Table 4. Initial decomposition temperature (Ti), temperature at which the weight reduction reaches 50 % (T50) and residual weight % (res %) for blends A, B, C and D.

Sample	Ti (°C)	T50 (°C)	res %	Sample	Ti (°C)	T50 (°C)	res %
1A	364.3	417.5	0.1	1C	355.0	396.0	1.3
1B	360.0	402.1	3.0	1D	355.0	400.0	2.6
2A	317.5	376.9	1.7	2C	166.0	399.0	0.7
2B	342.7	392.1	1.4	2D	220.0	400.0	0.5
3A	290.7	362.9	1.2	3C	170.0	395.0	0.0
3B	235.9	383.8	2.8	3D	220.0	397.5	11.0
4A	275.5	350.3	1.1	4C	170.0	390.0	0.8
4B	220.0	382.6	5.1	4D	200.0	396.0	5.5
5A	258.7	342.6	2.7	5C	160.0	381.0	1.4
5B	220.0	365.0	4.2	5D	220.0	390.0	10.0
6A	241.3	337.0	2.3	6C	160.0	260.0	0.4
6B	211.2	324.5	1.3	6D	223.0	372.5	5.4
7A	240.8	330.8	4.2	7C	150.0	230.0	1.6
7B	207.0	288.7	0.5	7D	200.0	265.0	3.2
8A	222.9	316.0	5.1	8C	150.0	222.0	1.0
8B	203.7	254.9	2.6	8D	200.0	260.0	4.4
9A	216.4	298.6	1.2	9C	140.0	202.0	4.3
9B	200.8	264.6	4.0	9D	200.0	249.0	5.6
10A	210.3	291.1	10.5	10C	140.0	195.0	1.6
10B	200.0	258.7	2.4	10D	200.0	248.0	7.9
11A	213.7	275.3	12.1	11C	140.0	190.0	2.2
11B	186.9	246.9	5.6	11D	200.0	265.0	0.0

Thermogravimetric analysis was carried out before calorimetric analysis for setting up the higher temperatures programmed in the DSC to avoid decomposition of the samples. From the Ti values presented in Table 4, the final temperatures of the first heating were determined (Experimental section/DSC measurements) since the obtaining of calorimetric information from the DSC thermograms requires the thermal stability of samples.

In addition, T50 values, usually used as thermal stability criterion, were represented against the LMWC content. This behavior can be observed in Figure 7 for blends A, B, C and D. The interaction of both TDP and MDP with P4VPy (blends A and B) and of both 22BP and 44BP with P2VPy (blends C and D) produces a decreasing in the thermal stability of the polymers as the LMWC content increases.

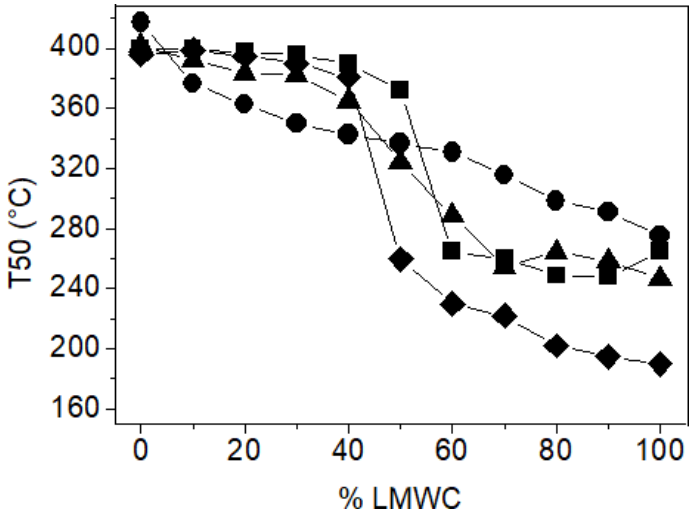

Figure 7. Variation of T50 with the composition for the blends A(●), B(▲), C(◆) and D(■).

Scanning Electron Microscopy was used as an additional and complementary technique to characterize blends A, B, C and D. Figure 8 shows micrographs obtained by SEM for selected compositions of blend C as examples. As it has been reported previously by our laboratory for similar systems [50-53], polymer component (P2VPy or 1C) shows a homogeneous surface and a trend to the formation of beads and bumpy textures, classic traits of crystalline LMWCs, is observed as the blend is richer in 22BP.

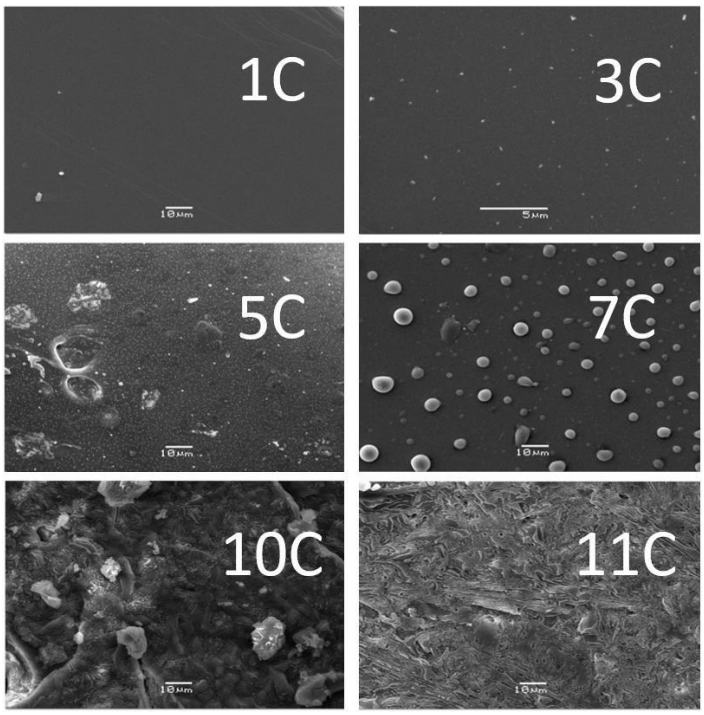

Figure 8. SEM micrographs for blend C (compositions 1C, 3C, 5C, 7C, 10C and 11C).

CONCLUSIONS

The addition of TDP and MDP to P4VPy and of 22BP and 44BP to P2VPy leads to an increase in the wave number corresponding to the deformation absorption of pyridine rings in P4VPy and P2VPy. This experimental behavior detected by FTIR reflects the increase in the stiffness of the pyridinic groups due to the formation of hydrogen bonding between LMWCs and polymers. Higher wave number values were observed for blends A and B as a consequence of the better steric availability of P4VPy to form hydrogen bonds.

DSC analysis shows that the addition of TDP and MDP produces a plasticizing effect in P4VPy, i.e., a decreasing of the Tg values, attributed to a good degree of interactions between the components. This effect was not observed for blends of 22BP and 44BP with P2VPy due to a lower level of molecular affinity also observed by FTIR. It was further noted that Tm and ΔH_{fus} of LMWCs decrease in all blends studied as the polymer content increases: crystallinity of TDP, MDP, 22BP and 44BP is progressively disrupted when they interact with the polymers.

Thermal decomposition profiles obtained by TGA show that the thermal stability of P4VPy and P2VPy is affected by the presence of LMWCs: T50 decreases with the increase of the LMWC content. Furthermore, the molecular affinity detected between the components produces morphological changes observed by SEM.

Specific intermolecular interactions such as hydrogen bonding were detected between functionalized vinyl polymers and LMWCs, which allow the obtaining of miscible systems.

ACKNOWLEDGEMENTS

The authors thank the Universidad de Concepción, scientific research grant 212.024.038-1.0, for financial support.

REFERENCES

1. G. Belorgey, R. E. Prud'Homme, *J. Polym. Sci. Polym. Phys.* 20, 191, (1982).
2. M. M. Coleman, A. W. Lichkus, P. C. Painter, *Macromolecules* 22, 586, (1989).
3. M. Rocha, *Rev. Plást. Mod*. 440, 149, (1993).
4. H. Mok Lee, O. Ok Park, *J. Rheol.* 38, 1405, (1994).
5. R. Kirk, D. Othmer, "Encyclopedia of Chemical Technology", John Wiley & Sons, 4th Edition, vol. 7, p. 349; vol. 19, p. 1108 (1993).
6. J. Areizaga, M. Milagros Cortázar, J. Elorza, J. Iruin, "Polímeros", Síntesis S. A., Madrid, Spain, chapter 12 (2002).
7. A. Taha, M. Magida, E. Shehata, *J. Appl. Polym. Sci.* 126, 1822, (2012).
8. J. He, F. Liu, Y. Luo, D. Jia, *J. Appl. Polym. Sci.* 126, 1527, (2012).
9. Z. Yang, K. Nollenberger, J. Albers, D. Craig, S. Qi, *Mol. Pharmaceutics* 10, 2767, (2013).
10. S. Djellali, T. Sadoun, N. Haddaoui, A. Bergeret, *Polym. Bull.* 72, 1177, (2015).
11. E. Laredo, D. Newman, R. Pezzoli, A. J. Müller, A. Bello, *J. Polym. Sci. Polym. Phys.* 54, 680, (2016).
12. J. Y. Lee, P. C. Painter, M. M. Coleman, *Macromolecules* 21, 346, (1988).
13. D. J. T. Hill, A. K. Whittaker, K. W. Wong, *Macromolecules* 32, 5285, (1999).
14. M. Urzúa, L. Gargallo, D. Radic´, *J. Appl. Polym. Sci.* 84, 1245, (2002).
15. L. T. Lee, E. M. Woo, *J. Polym. Sci. Polym. Phys.* 44, 1339, (2006).
16. J. Kratochvíl, A. Šturcová, A. Sikora, J. Dybal, *J. Polym. Sci. Polym. Phys.* 49, 1031, (2011).
17. E. Zuza, A. Lejardi, E. Meaurio, J. R. Sarasua, *Eur. Polym. J.* 63, 58, (2015).
18. S. Vicini, M. Castellano, E. Princi, *Polym. Bull.* 72, 743, (2015).
19. A. Lejardi, J. R. Sarasua, A. Etxeberria, E. Meaurio, *J. Polym. Sci. Polym. Phys.* 54, 1217, (2016).
20. E. S. Lopes, E. Domingos, R. S. Neves, W. Romão, K. R. de Souza, R. Valaski, B. S. Archanjo, F. G. Souza Jr., A. M. Silva, A. Kuznetsov, J. R. Araujo, *Eur. Polym. J.* 85, 588, (2016).
21. S. Matsushima, A. Takano, Y. Matsushita, *J. Polym. Sci. Polym. Phys.* 55, 1791, (2017).
22. G. Singh, H. Bhunia, A. Rajor, V. Choudhary, *Polym. Bull.* 66, 939, (2011).
23. M. Hazarika, T. Jana, *Eur. Polym. J.* 49, 1564, (2013).
24. D. Wu, W. Li, Y. Hao, Z. Li, H. Yang, H. Zhang, H. Zhang, L. Dong, *Polym. Bull.* 72, 851, (2015).
25. M. N. Tamaño-Machiavello, B. Bracke, C. M. Costa, S. Lanceros- Mendez, R. Sabatier i Serra, J. L. Gómez, *J. Polym. Sci. Polym. Phys.* 54, 672, (2016).
26. G. Liu, G. Qiu, *Polym. Bull.* 70, 849, (2013).
27. R. Avolio, R. Castaldo, G. Gentile, V. Ambrogi, S. Fiori, M. Avella, M. Cocca, M. E. Errico, *Eur. Polym. J.* 66, 533, (2015).
28. K. Zhang, Q. Zhang, H. Zhang, J. Shen, Q. Niu, R. Xia, *Macromol. Chem. Phys.* 219, 1700527, (2018).
29. H. T. Oyama, Y. Tanaka, S. Hirari, S. Shida, A. Kadosaka, *J. Polym. Sci. Polym. Phys.* 49, 342, (2011).
30. R. Kirk, D. Othmer, "Encyclopedia of Chemical Technology", John Wiley & Sons, 4th Edition, vol. 2, p. 18; vol. 3, p. 435 (1993).
31. X. Wang, Y. Zhuang, L. Dong, *J. Appl. Polym. Sci.* 126, 1876, (2012).

32. L. Silva, S. Tognana, W. Salgueiro, *J. Polym. Sci. Polym. Phys.* 51, 680, (2013).
33. M. J. Mochane, A. S. Luyt, *Polym. Bull.* 72, 2263, (2015).
34. T. P. Gumede, A. S. Luyt, R. A. Pérez-Camargo, A. Iturrospe, A. Arbe, M. Zubitur, A. Mugica, A. J. Müller, *J. Polym. Sci. Polym. Phys.* 54, 1469, (2016).
35. Y. J. Chen, A. Huang, T. Ellingham, C. Chung, L. S. Turng, *Eur. Polym. J.* 98, 262, (2018).
36. G. Carini Jr., G. Carini, G. D'Angelo, M. Federico, G. Di Marco, A. Bartolotta, *J. Polym. Sci. Polym. Phys.* 56, 340, (2018).
37. A. H. Suzuki, B. G. Botelho, L. S. Oliveira, A. S. Franca, *Eur. Polym. J.* 99, 142, (2018).
38. G. Y. Liu, L. P. Lv, C. J. Chen, X. F. Hu, J. Ji, *Macromol. Chem. Phys.* 212, 643, (2011).
39. L. Garber, N. Jingar, R. Rosario-Meléndez, K. E. Uhrich, *J. Polym. Sci. Polym. Phys.* 53, 685, (2015).
40. H. Wang, Y. Wu, G. Liu, Z. Du, X. Cheng, *Macromol. Chem. Phys.* 217, 2004, (2016).
41. M. Szabó, B. Berke, K. László, Z. Osváth, A. Domján, *Eur. Polym. J.* 93, 750, (2017).
42. F. M. Rabagliati, M. Saavedra, P. Galvez, D. A. Canales, G. P. Orihuela, P. A. Zapata, H. G. Cárdenas, *Polym. Bull.* 75, 415, (2018).
43. A. E. Mercado-Pagán, Y. Kang, D. F. E. Ker, S. Park, J. Yao, J. Bishop, Y. P. Yang, *Eur. Polym. J.* 49, 3337, (2013).
44. S. More, R. Dhokne, S. Moharil, *Polym. Bull.* 75, 909, (2018).
45. A. Hayder, A. Hussain, A. N. Khan, H. Waheed, *Polym. Bull.* 75, 1197, (2018).
46. A. Al-Mulla, K. Alfadhel, G. Qambar, H. Shaban, *Polym. Bull.* 70, 2599, (2013).
47. A. Woz´niak-Braszak, K. Jurga, G. Nowaczyk, M. Dobies, M. Szostak, J. Jurga, S. Jurga, *Eur. Polym J.* 64, 62, (2015).
48. D. Garcia-Garcia, E. Rayón, A. Carbonell-Verdu, J. Lopez-Martinez, R. Balart, *Eur. Polym. J.* 86, 41, (2017).
49. A. Rigoussen, P. Verge, J. M. Raquez, Y. Habibi, P. Dubois, *Eur. Polym. J.* 93, 272, (2017).
50. N. Gatica, N. Alvarado, D. Sepúlveda, *J. Chil. Chem. Soc.* 51, 945, (2006).
51. N. Gatica, N. Alvarado, *J. Chil. Chem. Soc.* 54, 317, (2009).
52. N. Gatica, O. Monares, *J. Chil. Chem. Soc.* 55, 399, (2010).
53. N. Gatica, L. Soto, C. Moraga, L. Vergara, *J. Chil. Chem. Soc.* 58, 2048, (2013).
54. M. A. Llorente, A. Horta, "Técnicas de caracterización de polímeros", UNED Ediciones, Madrid, Spain, chapter 5 (1991).
55. L. Cesteros, *Revista Iberoamericana de Polímeros* 5, 111, (2004).
56. J. Li, Y. He, Y. Inoue, *J. Polym. Sci. Polym. Phys.* 39, 2108, (2001).
57. Y. He, N. Asakawa, Y. Inoue, *Macromol. Chem. Phys.* 202, 1035, (2001).